

Chapter 11

CQED

Abstract In this chapter we will discuss two different physical systems in which a single mode of the electromagnetic field in a cavity interacts with a two-level dipole emitter. In the first example, the system is comprised of a single two-level atom inside an optical cavity. The study of this system is often known as cavity quantum electrodynamics (cavity QED) as it may be described using the techniques of the previous chapter.

The second example is comprised of a superconducting Cooper pair box inside a co-planar microwave resonator. The description of this system is given in terms of the quantisation of an equivalent electronic circuit and thus goes by the name of circuit quantum electrodynamics (circuit QED).

In both cases we are typically interested in the *strong coupling regime* in which the single photon Rabi frequency g (the coupling constant in the Jaynes–Cummings model) is larger than both the spontaneous decay rate, γ , of the two-level emitter and the rate, κ , at which photons are lost from the cavity.

11.1 Cavity QED

The primary difficulty we face in cavity QED is finding a way to localise a single two-level atom in the cavity mode for long time intervals. One approach, pioneered by the Caltech group of Kimble [1], is to first trap and cool two-level atoms in a magneto-optical trap (MOT) (see Chap. 18) and then let them fall into a high finesse cavity placed directly below the MOT. If the geometry is correctly arranged then at most one atom will slowly fall through the cavity at a time. Another approach is to use constraining forces to trap a single atom in the optical cavity. This can be done using the light shift forces of a far off resonant laser field on a two-level atom [2, 3] (see Chap. 18), or it can be done using an ion trap scheme [4] (see Chap. 17). A very novel way to get atoms from the MOT into the cavity deterministically has been pioneered by the Chapman group in Georgia [5]. They use an optical dipole standing wave trap as a kind of atomic conveyor belt to move atoms from the MOT into the cavity.

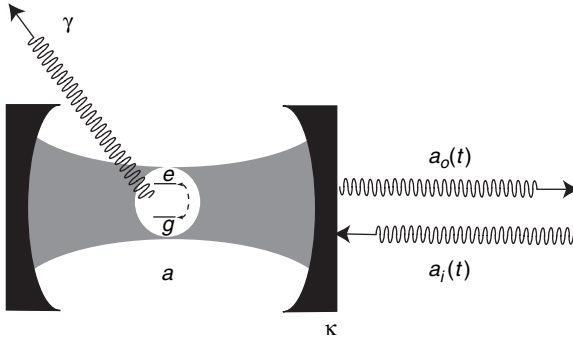


Fig. 11.1 A cavity QED scheme: a single two-level dipole emitter is fixed at a particular location inside a Fabry-Perot cavity. The dipole is strongly coupled to a single cavity mode, a , but can emit photons at rate γ into external modes. Photons are emitted from the end mirror of the cavity at rate κ

Consider the scheme in Fig. 11.1. The interaction Hamiltonian between a single two-level atom at the point \vec{x} in a Fabry-Perot cavity is given by

$$H_I = g(\vec{x})a^\dagger\sigma_+ + g^*(\vec{x})a\sigma_- \quad (11.1)$$

where

$$g(\vec{x}) = \left(\frac{\mu^2 \omega_c}{2\hbar \epsilon_0 V} \right)^{1/2} U(\vec{x}) \equiv g_0 U(\vec{x}) \quad (11.2)$$

This is obtained from (10.17) with the traveling wave mode function replaced by a cavity standing wave mode function, $U(\vec{x})$. Here μ is the dipole moment for the two-level system and V is the cavity mode volume defined by $V = \int \sin^2 |U(\vec{x})|^2 d^3x$.

Let us consider the interaction between a single cavity mode and a two-level system. For the present we neglect the spatial dependance of $g(\vec{x})$. The master equation, in the interaction picture, for a single two-level atom interacting with a single cavity mode, at optical frequencies, is

$$\begin{aligned} \frac{d\rho}{dt} = & -i\delta[a^\dagger a, \rho] - i\frac{\Delta}{2}[\sigma_z, \rho] - i[\epsilon^* a + \epsilon a^\dagger, \rho] - ig[a\sigma_+ + a^\dagger\sigma_-, \rho] \\ & + \frac{\kappa}{2}(2a\rho a^\dagger - a^\dagger a\rho - \rho a^\dagger a) + \frac{\gamma}{2}(2\sigma_- \rho \sigma_+ - \sigma_+ \sigma_- \rho - \rho \sigma_+ \sigma_-) \end{aligned} \quad (11.3)$$

where ϵ represents a classical coherent laser field driving the cavity mode at frequency ω_L , the detuning between the cavity field and the driving field is $\delta = \omega_c - \omega_L$ and $\Delta = \omega_a - \omega_L$ is the detuning between the two-level system and the driving field. From this equation we can derive equations for first order field/atom moments;

$$\frac{d\langle a \rangle}{dt} = -\left(\frac{\kappa}{2} + i\delta \right) \langle a \rangle - i\epsilon - ig\langle \sigma_- \rangle \quad (11.4)$$

$$\frac{d\langle \sigma_- \rangle}{dt} = -\left(\frac{\gamma}{2} + i\Delta \right) \langle \sigma_- \rangle + ig\langle a\sigma_z \rangle \quad (11.5)$$

$$\frac{d\langle\sigma_z\rangle}{dt} = -\gamma(\langle\sigma_z\rangle + 1) - 2ig(\langle a\sigma_+\rangle - \langle a^\dagger\sigma_-\rangle) \quad (11.6)$$

Looking at these equations we see that we do not get a closed set of equations for the first order moments, for example the equation for $\langle\sigma_-\rangle$ is coupled to $\langle a\sigma_z\rangle$. A number of procedures have been developed to deal with this. If there are many atoms interacting with a single mode field, an expansion in the inverse atomic number can be undertaken and we will describe this approach in Sect. 11.1.3. However a good idea of the behaviour expected can be obtained simply by factorising all higher order moments. This of course neglects quantum correlations and is thus not expected to be able to give correct expressions for, say, the noise power spectrum of light emitted from the cavity. Nonetheless it is often a good place to start as it captures the underlying dynamical structure of the problem. We thus define the *semiclassical* equations as

$$\dot{\alpha} = -\frac{\tilde{\kappa}}{2}\alpha - i\varepsilon - igv \quad (11.7)$$

$$\dot{v} = -\frac{\tilde{\gamma}}{2}v + ig\alpha z \quad (11.8)$$

$$\dot{z} = -2ig(\alpha v^* - \alpha^*v) - \gamma(z + 1) \quad (11.9)$$

where the dot signifies differentiation with respect to time and

$$\tilde{\kappa} = \kappa + 2i\delta \quad (11.10)$$

$$\tilde{\gamma} = \gamma + 2i\Delta \quad (11.11)$$

The first thing to consider is the steady state solutions, α_s, z_s, v_s which are given implicitly by

$$z_s = -\left[1 + \frac{n}{n_0(1 + \Delta_1^2)}\right]^{-1} \quad (11.12)$$

$$\alpha_s = -\frac{2i\varepsilon}{\tilde{\kappa}} \left[1 + \frac{2C(1 + i\phi)^{-1}(1 + i\Delta_1)^{-1}}{1 + \frac{n}{n_0(1 + \Delta_1^2)}}\right]^{-1} \quad (11.13)$$

$$v_s = \frac{2ig}{\tilde{\gamma}}\alpha_s z_s \quad (11.14)$$

where

$$n = |\alpha_s|^2 \quad (11.15)$$

is the steady state intracavity intensity and

$$\phi = 2\delta/\kappa \quad (11.16)$$

$$\Delta_1 = 2\Delta/\gamma \quad (11.17)$$

$$n_0 = \frac{\gamma^2}{8g^2} \quad (11.18)$$

$$C = \frac{2g^2}{\kappa\gamma} \quad (11.19)$$

The parameter n_0 sets the scale for the intracavity intensity to saturate the atomic inversion and is known as the *critical* photon number. The parameter C is sometimes defined in terms of the critical atomic number, N_0 , as $C = N_0^{-1}$. Why this name is appropriate is explained in Sect. 11.1.3 where we consider cavity QED with many atoms.

We can now determine how the steady state intracavity intensity depends on the driving intensity. We first define the scaled driving intensity and intracavity intensity by

$$I_d = \frac{4\varepsilon^2}{\kappa^2 n_0} \quad (11.20)$$

$$I_c = \frac{n}{n_0} \quad (11.21)$$

The driving intensity and the intracavity intensity are then related by

$$I_d = I_c \left[\left(1 + \frac{2C}{1 + \Delta_1^2 + I_c} \right)^2 + \left(\phi - \frac{2C\Delta_1}{1 + \Delta_1^2 + I_c} \right)^2 \right] \quad (11.22)$$

The phase θ_s of the steady state cavity field is shifted from the phase of the driving field (here taken as real) where

$$\tan \theta_s = - \frac{\phi - 2\Delta_1 C / (1 + \Delta_1^2 + I_c)}{1 + 2C / (1 + \Delta_1^2 + I_c)} \quad (11.23)$$

Equation (11.22) is known as the *bistability state equation*, a name that makes sense when we plot the intracavity intensity versus the driving intensity, see Fig. 11.2. It can be shown that the steady state corresponding to those parts of the curve with

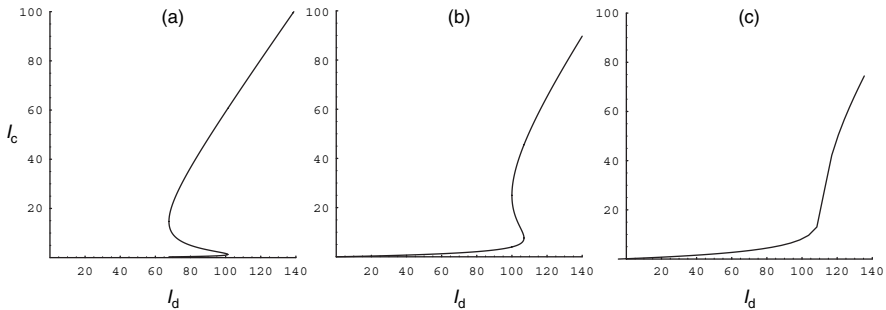


Fig. 11.2 The intracavity intensity versus the driving intensity, as given implicitly by (11.22), for various values of the detuning between the atom and the driving field. In all cases we assume the driving is on resonance with the cavity so that $\phi = 0$ and $C = 9$. (a) $\Delta_1 = 0$, (b) $\Delta_1 = 2$, (c) $\Delta_1 = 3$

negative slope are unstable. Clearly there are regions for which two stable steady states coexist for a given driving intensity.

Cavity QED requires that we are in the *strong coupling* limit in which $g_0 > \gamma, \kappa$. Furthermore a necessary condition for strong coupling is that $(n_0, N_0) \ll 1$. In this limit a single photon in the photon can lead to significant dynamics. One way to make g_0 large is to use a very small mode volume V and a large dipole moment. In recent years, with optical Fabry-Perot cavities, it has been possible to achieve $n_0 \approx 10^{-3}$ – 10^{-4} and $N_0 \approx 10^{-2}$ – 10^{-3} . The mirrors of these cavities are highly reflective, with reflectivity coefficients greater than 0.999998. This means that the inter mirror spacing can be made very small giving a small mode volume. Typical parameters for the Caltech group of Kimble, using atomic cesium, are [1]

$$(g_0, \kappa, \gamma) = (34, 2, 1.25) \text{ MHz} \quad (11.24)$$

which give critical parameters $n_0 = 0.0029$ and $N_0 = 0.018$. Even better performance is possible using microtoroidal resonators, again implemented by the Caltech group [6], or excitonic dipoles in quantum dots integrated into photonic band gap materials, implemented by the Imamoglu group in Zurich [7]. A very different approach is to use Rydberg atoms, which have very large dipole moments, in superconducting microwave cavities. This approach has been pioneered by the group of Haroche in Paris [8].

11.1.1 Vacuum Rabi Splitting

With the ability to trap a single atom in the cavity and cool it to very low kinetic energies, it becomes possible to measure the vacuum Rabi splitting. This is the splitting energy, induced by the interaction in (11.1), of the degenerate states $|n=0\rangle|e\rangle, |n=1\rangle|g\rangle$ where $a^\dagger a|n\rangle = n|n\rangle$ is a photon number eigenstate for the intracavity field. As we saw in Chap. 10, Sect. 10.2, these states are split in energy by $2g$. If g is large enough an excited atom is likely to emit a single photon into the cavity mode and periodically reabsorb and reemit before the excitation is lost.

Boca et al. [9] observed the vacuum Rabi splitting using a single Cs atom trapped inside an optical Fabry-Perot cavity using a far off-resonance optical dipole trap. An important breakthrough that enabled this experiment was the ability to cool the atom (see Chap. 18) using a Raman cooling scheme for motion of the atom along the cavity axis. The inferred uncertainties in the axial and transverse position of the atom in the trap were $\Delta z_{\text{ax}} \approx 33 \text{ nm}$ and $\Delta r_{\text{trans}} \approx 5.5 \mu\text{m}$. The two electronic levels used were the $6S_{1/2}, F=4 \rightarrow 6P_{3/2}, F'=5$ transition of the $D2$ with a maximum single photon Rabi frequency of $2g_0/2\pi = 68 \text{ MHz}$. The transverse atomic decay rate is $\gamma/2\pi = 1.3 \text{ MHz}$ and the cavity decay rate is $\kappa/2\pi = 2.05 \text{ MHz}$. Clearly this is in the strong coupling regime.

A weak probe laser beam is incident on the cavity with a frequency ω_p that can be tuned through the atomic resonance frequency. The transmitted light is detected

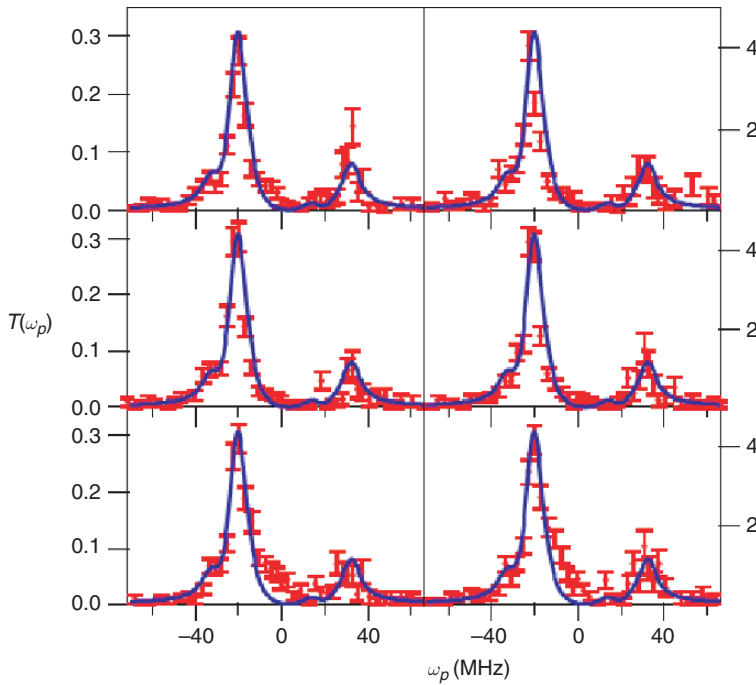


Fig. 11.3 The results of a measurement of the vacuum Rabi splitting performed by the Caltech group. Six different studies are shown, together with a comparison to theory (*solid line*). From [9]

at a photodetector and thus the transmission coefficient $T(\omega_p)$ can be measured. The results for six cases in which one atom was present in the cavity are shown in Fig. 11.3. Also shown as a solid line is the theoretical prediction based on the steady state solution to the master equation. The asymmetry of the peaks is due to the different Stark shifts for the Zeeman sub-levels of the excited state and optical pumping.

11.1.2 Single Photon Sources

In Chap. 16 we discuss how single photons can be used to encode and process information in a fully quantum coherent fashion. To realise such scheme however requires a very special kind of light source that produces a train of transform limited pulses each containing one and only one photon with high probability. Cavity QED schemes can be used to generate such states. If an atom, coupled to a single mode cavity field, was prepared in the excited state at time $t = t_0$, it will emit a photon into the cavity on a time scale determined by g^{-1} . If we are in the strong coupling regime, this photon will be reabsorbed by the atom on the same time scale. This is not what

we want for a single photon source. In order to ensure the photon is emitted from the cavity a time $t = t_0 + \tau$, we will need a bad cavity, i.e. one for which $\kappa \gg g, \gamma$. We also need to ensure that the atom does not emit a photon in any mode other than the cavity mode, so that we require $g \gg \gamma$. The net effect is that the rate for the photon to be emitted preferentially into the output mode from the cavity is much greater than its free-space spontaneous emission rate. This is known as the Purcell effect.

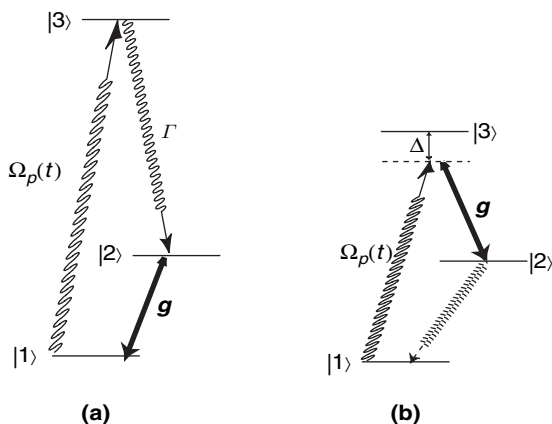
Of course there is still some uncertainty in the emission of the photon from the cavity as this is a Poisson process at rate κ and T is a random variable. The probability density for T is

$$p(T) = \kappa e^{-\kappa T} \quad (11.25)$$

This has a mean given by κ^{-1} , which also happens to be the uncertainty in the emission time. Such a system necessarily has some “time jitter” in the single photon pulses emitted from the cavity. Once the photon is emitted, we need to re-excite the atom to generate another pulse. Let us suppose that the repetition time for this is T . If we can arrange things so that $T \gg \kappa^{-1}$, the relative time jitter is small.

Of course the excitation itself is a dynamical process and takes some time. There is some time scale associated with this excitation and the excitation pulse itself may have some non trivial time dependence. There are two models of interest for the excitation process. In the first model, a strong classical pump pulse excites a multi level atomic system which then decays *non radiatively* into the excited state of the dipole coupled to the cavity mode, see Fig. 11.4 (a). The problem with this scheme is that the entry of the system into the excited state $|e\rangle$ is a random process (likely a Poisson process). One might think this will cause no problems so long as Γ is large enough. However the condition $g \gg \gamma$ means that these fluctuations are important when the Purcell effect becomes large [10]. In the second model, (b), the classical pulsed field together with the cavity field excites a two photon Raman transition to state $|2\rangle$. The effective interaction Hamiltonian between the field and the atom is

Fig. 11.4 Two schemes for a single photon source via cavity QED. In (a), a pulsed optical field excites the system to an auxiliary excited state (or states), which then decays non radiatively into the excited state $|e\rangle$. The transition $|1\rangle \leftrightarrow |2\rangle$ is coupled to a cavity mode with coupling constant g . In (b) the pulsed field together with the cavity field excites a two photon Raman transition to state $|2\rangle$.



$$H_1(t) = \hbar \frac{\Omega_p(t)g}{\Delta} (a^\dagger |2\rangle\langle 1| + a |1\rangle\langle 2|) \quad (11.26)$$

In effect, the coupling of the atom to the cavity field has become time dependent through the dependance on the pump field, $\omega_p(t)$.

In Fig. 11.5 we show the results of simulation for scheme (a) [11]. We assume that the pump pulse excitation is instantaneous. The quality of such a single

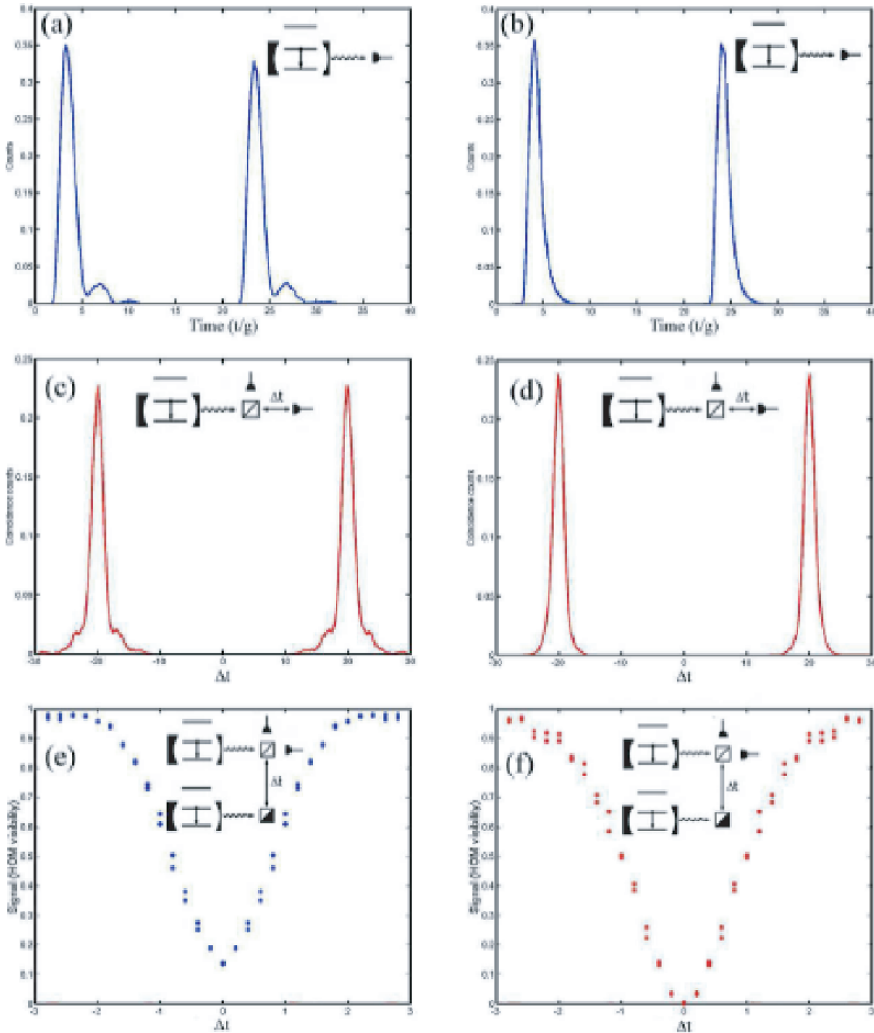


Fig. 11.5 The probability to detect a single photon per unit time for scheme (a) in Fig. 11.4. The instantaneous pump pulses are applied at times marked by the arrow. In (a) g is sufficiently large that the photon can be exchanged between the cavity field and atom before emission. In (b) however $\kappa > g$ and the photon emission is dominated by a Poisson decay process. Also shown are the corresponding results for a simulated $g^{(2)}(\tau)$ experiment (c, d) and a HOM coincidence experiment (e, f)

photon source can be operationally determined by two experiments: a Hanbury-Brown/Twiss experiment to measure $g^{(2)}(\tau)$ and a Hong-Ou-Mandel two-photon interference experiment (see Sect. 16.4.2). If we do indeed have a source of single photon pulses with one and only one photon per pulse $g^{(2)}(\tau)$ should be zero at zero delay and peak at the pulse repetition rate. Like wise if we mode match two identical single photon pulses on a 50/50 beam splitter as in the Hong-Ou-Mandel two-photon interference experiment, the coincidence rate for zero delays between the pulses should go to zero. Clearly we do not want to be in a regime where significant Rabi oscillations can occur before photon emission.

The second scheme, (b), has been implemented by *Keller et al.* [4] using a ion trap CQED scheme. They used a laser cooled Ca^+ ion confined to the centre of an optical cavity with a linear RF trap. The levels are given as $|1\rangle \rightarrow 4^2S_{1/2}$, $|2\rangle \rightarrow 3^2D_{3/2}$, $|3\rangle \rightarrow 4^2P_{1/2}$. The pump pulse had a carrier wavelength of 397 nm while the Raman resonance was tuned to the cavity resonant wavelength of 866 nm. The single photon Rabi frequency was $g/2\pi = 0.92$ MHz. The spontaneous decay rate of the $P_{1/2} \rightarrow D_{3/2}$ transition was $\gamma/2\pi = 1.69$ MHz and the cavity decay rate was $\kappa/2\pi = 1.2$ MHz. The Raman pump pulse had a predefined intensity profile of up to 6 ms duration and was repeated at a rate of 100 kHz. An interesting feature of the experiment was that the temporal shape of the pump pulse could be controlled to some extent. The output from the cavity is then directed towards a avalanche photodiode detector with overall detection efficiency of about $\eta = 0.05$. The time of each photodetection event is recorded with a 2 ns resolution and the resulting arrival time distribution gives the detection probability per unit time, $n(t)$ for the single photon (with $n(t) = \eta \langle a^\dagger(t)a(t) \rangle$, see Sect. 16.4.2). The results are shown in Fig. 11.6 for various choices for the temporal structure of the pump pulse. Also shown is a full simulation of $n(t)$ based on the master equation. *Keller et al.* also measured the cross correlation events in a Hanbury-Brown/Twiss experiment. The peak suppression at zero delay was by a factor of the order of 10^5 compared to the counts in all the other peaks.

11.1.3 Cavity QED with N Atoms

There are a large class of experiments in which more than one atom (for example in an atomic vapour) interacts with a single cavity mode. In that case a single cavity photon is *shared* over many atomic excitations, and so the effect on any single atom is reduced. In this case we might expect that an approximate scheme based on an expansion in N^{-1} where N is the number of atoms involved, might be possible. We will present one approach to this problem developed by *Drummond* and *Walls* [12].

The interaction Hamiltonian in (11.1) becomes

$$H_I = g_0 \sum_{j=1}^N a^\dagger \sigma_-^{(j)} e^{i\vec{k} \cdot \vec{x}_j} + a \sigma_+^{(j)} e^{-i\vec{k} \cdot \vec{x}_j} \quad (11.27)$$

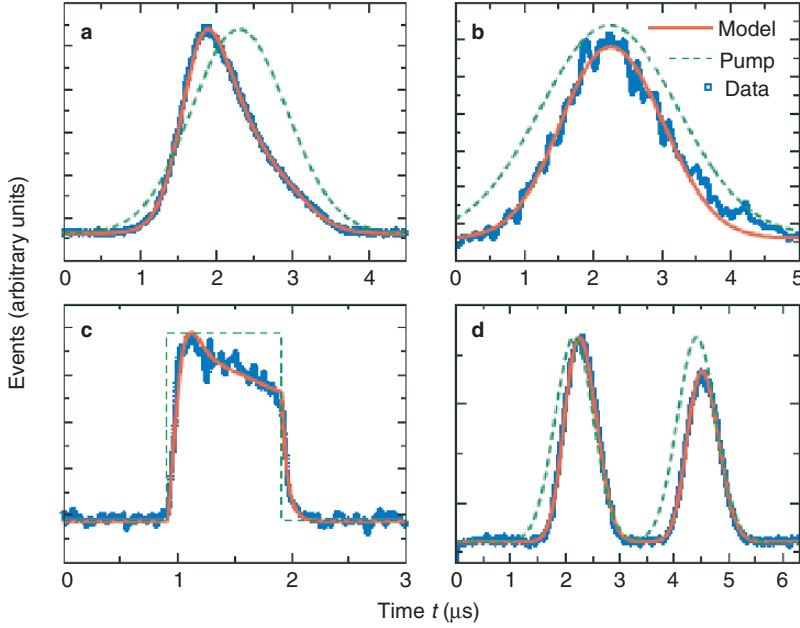


Fig. 11.6 The probability to detect a single photon per unit time, versus time, for scheme (b) in the experiment of *Keller et al.* [5], with various pump pulse shapes (*dashed line*): (a), Strong Gaussian pump; (b), Weak Gaussian pump; (c), Square-wave pump; (d), Double-peaked pump

$$= g(a^\dagger S + a S^\dagger) \quad (11.28)$$

where we have used plane wave modes to be specific, and where we have defined the collective atomic polarisation operators as

$$S = \sum_{j=1}^N \sigma_-^{(j)} e^{i\vec{k} \cdot \vec{x}_j} \quad (11.29)$$

This immediately suggests that we should also define the collective atomic inversion operator

$$D = \sum_{j=1}^N \sigma_z^{(j)} \quad (11.30)$$

These operators obey the following commutation relations,

$$[S^\dagger, S] = D \quad (11.31)$$

$$[D, S] = -2S \quad (11.32)$$

$$[D, S^\dagger] = 2S^\dagger \quad (11.33)$$

We assume that each atom undergoes independent spontaneous emission out of the cavity mode and that such emitted photons are not reabsorbed. The master equation then takes the form

$$\begin{aligned} \frac{d\rho}{dt} = & -i\delta[a^\dagger a, \rho] - i\frac{\Delta}{2}[D, \rho] - i[\epsilon^* a + \epsilon a^\dagger, \rho] - i g[a^\dagger S + a S^\dagger, \rho] \\ & + \frac{\kappa}{2}(2a\rho a^\dagger - a^\dagger a\rho - \rho a^\dagger a) \\ & + \frac{\gamma}{2} \sum_{j=1}^N (2\sigma_-^{(j)} \rho \sigma_+^{(j)} - \sigma_+^{(j)} \sigma_-^{(j)} \rho - \rho \sigma_+^{(j)} \sigma_-^{(j)}) \end{aligned} \quad (11.34)$$

We next define the normally ordered characteristic function

$$\chi(\vec{\lambda}) = \text{Tr}\{\rho \Xi(\vec{\lambda})\} \quad (11.35)$$

where

$$\Xi(\vec{\lambda}) = e^{i\lambda_5 S^\dagger} e^{i\lambda_4 D} e^{i\lambda_3 S} e^{i\lambda_2 a^\dagger} e^{i\lambda_1 a} \quad (11.36)$$

with $\vec{\lambda}^T = (\lambda_1, \lambda_2, \lambda_3, \lambda_4, \lambda_5)$. The positive P -representation for the atom-field state is then defined as the multi-dimensional Fourier transform of the characteristic function,

$$P(\vec{\alpha}) = \frac{1}{(2\pi)^5} \int \chi(\vec{\lambda}) e^{-i\vec{\lambda} \cdot \vec{\alpha}} d^5 \lambda \quad (11.37)$$

where $\vec{\alpha}^T = (\alpha, \beta, v, D, u)$.

To obtain an equation of motion for $P(\vec{\alpha})$ we first need to find an equation of motion for the characteristic function, $\chi(\vec{\lambda})$ and then integrate by parts. Consider, for example, the term arising from the interaction with the cavity field mode,

$$\left(\frac{d\chi}{dt} \right)_I = -ig \langle [\Xi, a^\dagger S] \rangle - \langle [\Xi, a S^\dagger] \rangle \quad (11.38)$$

We can use the commutation relations for these operators to show that, for example,

$$\langle [\Xi, a S^\dagger] \rangle = \left(\lambda_1 \frac{\partial}{\partial \lambda_3} - (1 - e^{2i\lambda_4}) \frac{\partial^2}{\partial \lambda_2 \partial \lambda_3} - i\lambda_5 \frac{\partial^2}{\partial \lambda_2 \partial \lambda_4} + \lambda_5^2 \frac{\partial^2}{\partial \lambda_2 \partial \lambda_5} \right) \chi(\vec{\lambda}) \quad (11.39)$$

The corresponding term in the equation of motion for $P(\vec{\alpha})$ is

$$\left(\frac{\partial P}{\partial t} \right)_I = -ig \left(-\frac{\partial}{\partial \alpha} v + (1 - e^{-2\partial_D}) \beta v + \frac{\partial^2}{\partial u^2} \beta u - \frac{\partial}{\partial u} \beta D \right) P \quad (11.40)$$

$$+ ig \left(-\frac{\partial}{\partial \beta} u + (1 - e^{-2\partial_D}) \alpha u + \frac{\partial^2}{\partial v^2} \alpha v - \frac{\partial}{\partial v} \alpha D \right) P \quad (11.41)$$

where $\partial_D = \frac{\partial}{\partial D}$.

A problem is immediately apparent: this term contains infinite order derivatives and thus the resulting equation is not of Fokker–Planck form and does not define a stochastic process. However a careful analysis shows that the exponential may be truncated to second order in an asymptotic expansion in N^{-1} , which for $N \gg 1$ is a reasonable approximation. The result after truncating is

$$\begin{aligned} \frac{\partial P}{\partial t} = & [-\partial_\alpha[-i\varepsilon - \tilde{\kappa}\alpha/2 - igv] - \partial_v[ig\alpha D - \tilde{\gamma}v/2] \\ & - \partial_D[-\gamma(D+N) - 2ig(u\alpha - v\beta)] \\ & + \partial_v^2[ig\alpha v] + \partial_D^2[\gamma(D+N) - 2ig(u\alpha - v\beta)] + \text{CC}] P \end{aligned} \quad (11.42)$$

where CC stands for complex conjugate under the condition that $v^* \mapsto u$, $u^* \mapsto v$, $\alpha^* \mapsto \beta$, $\beta^* \mapsto \alpha$. The corresponding stochastic differential equations are

$$\begin{aligned} \dot{\alpha} &= -\tilde{\kappa}\alpha/2 - i\varepsilon - igv + \Gamma_\alpha \\ \dot{\beta} &= -\tilde{\kappa}^*\alpha/2 + i\varepsilon + igv + \Gamma_\beta \\ \dot{v} &= -\tilde{\gamma}v/2 + ig\alpha D + \Gamma_v \\ \dot{u} &= -\tilde{\gamma}^*u/2 - ig\beta D + \Gamma_u \\ \dot{D} &= -\gamma(D+N) - 2ig(\alpha u - \beta v) + \Gamma_D \end{aligned} \quad (11.43)$$

which should be compared to the single atom semiclassical equations to which they reduce when noise is neglected and we make the replacements $\beta \mapsto \alpha^*$, $u \mapsto v^*$, $N \mapsto 1$. The only non-zero noise correlation functions are

$$\langle \Gamma_v(t) \Gamma_v(t') \rangle = 2ig\alpha v \delta(t-t') \quad (11.44)$$

$$\langle \Gamma_u(t) \Gamma_v(t') \rangle = 2ig\alpha u \delta(t-t') \quad (11.45)$$

$$\langle \Gamma_D(t) \Gamma_D(t') \rangle = 2\gamma(D+N) - 4ig(\alpha u - \beta v) \delta(t-t') \quad (11.46)$$

These equations now provide a basis to obtain a phenomenological description of optical bistability in terms of an intensity dependent cavity detuning. To proceed we will assume that $\gamma \gg \kappa$ so that the atomic variables can be assumed to reach a steady state slaved to the instantaneous values of the field variables. This is called *adiabatic elimination*. The next step is to approximate the noise correlation functions for the atomic variables by replacing u, v by the steady state values of the deterministic equations for these variables. This is equivalent to a linearisation around the deterministic steady state. The validity of this approximation rests on $N \gg 1$. The resulting atomic variables are then substituted into the field equations to give

$$\dot{\alpha} = -i\varepsilon - \tilde{\kappa}\alpha/2 - \frac{2g^2 N \alpha}{\tilde{\gamma} \Pi(\alpha\beta)} + \Gamma(t) \quad (11.47)$$

where

$$\Pi(\alpha\beta) = 1 + \frac{\alpha\beta}{n_0(1 + \Delta_1^2)} \quad (11.48)$$

with n_0 the saturation photon number and Δ_1 as previously defined in (11.17 and 11.18).

$$\begin{aligned}\langle \Gamma(t)\Gamma(t') \rangle &= \frac{\kappa C x^2}{(1 + X + \Delta_1^2)^3} \left[(1 - i\Delta_1)^3 + \frac{X^2}{2} \right] \delta(t - t') \\ \langle \Gamma^\dagger(t)\Gamma(t') \rangle &= \frac{\kappa C x^2}{(1 + X + \Delta_1^2)^3} \left[2X + \frac{X^2}{2} \right] \delta(t - t')\end{aligned}\quad (11.49)$$

with $x = \alpha/\sqrt{n_0}$ and $X = \alpha\beta/n_0$.

11.2 Circuit QED

Superconducting coplanar microwave cavities [13] enable a new class of experiments in circuit quantum electrodynamics in the strong coupling regime [14]. The dipole emitter in this case is a single superconducting metallic island separated by tunnel junctions from a Cooper pair reservoir. Under appropriate conditions it is possible for the charge on the island to be restricted to at most a single Cooper pair. This Cooper pair tunneling on an off the island constitutes a single large electric dipole system.

A possible experimental implementation is shown in Fig. 11.7.

The coupling between a Cooper pair box charge system and the microwave field of circuit QED is given by [13]

$$H = 4E_c \sum_N (N - n_g(t))^2 |N\rangle\langle N| - \frac{E_J}{2} \sum_{N=0} (|N\rangle\langle N+1| + |N+1\rangle\langle N|) \quad (11.50)$$

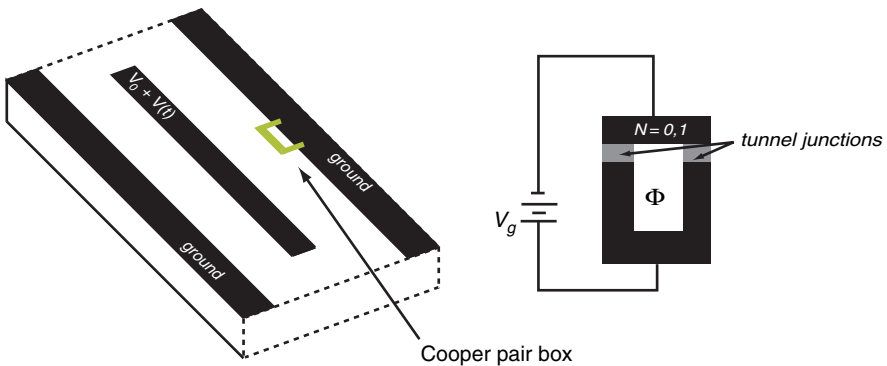


Fig. 11.7 A co-planar microwave resonator is coupled to a Cooper pair box electric dipole

where

$$E_C = \frac{e^2}{2C_\Sigma}$$

$$n_g(t) = \frac{C_g V_g(t)}{2e}$$

with C_Σ the capacitance between the island and the rest of the circuit, C_g is the capacitance between the CPB island and the bias gate for the island, and $V_g(t)$ is the total voltage applied to the island by the bias gate composed of a DC field, $V_g^{(0)}$ and microwave field in the cavity, $\hat{v}(t)$. Thus we can write $V_g(t) = V_g^{(0)} + \hat{v}(t)$, where the hat indicates a quantisation of the cavity field. Including the time dependent cavity field we can write

$$n_g(t) = n_g^{(0)} + \delta\hat{n}_g(t) \quad (11.51)$$

where

$$\delta\hat{n}_g(t) = \frac{C_g}{2e} \hat{v}(t) \quad (11.52)$$

The Hamiltonian in (11.50) is written in the Cooper pair number basis. In this basis the electrostatic energy of the first term is quite clear. The Josephson energy term describes tunneling of single Cooper pairs across the junction. This term is more traditionally (i.e. in mean-field theory) written in the phase representation as $E_J \cos \theta$. The connection between these two representations is discussed in [15].

If the Cooper pair box is sufficiently small, the electrostatic charging energy is so large that it is very unlikely that there will be more than a single Cooper pair on the island at any time. We can then usual restrict the CPB Hilbert space to $N = 0, 1$, we can write the Hamiltonian as

$$H = -2E_C(1 - 2n_g^{(0)})\bar{\sigma}_z - \frac{E_J}{2}\bar{\sigma}_x - 4E_C\delta\hat{n}_g(t)(1 - 2n_g^{(0)} - \bar{\sigma}_z) \quad (11.53)$$

where $\bar{\sigma}_z = |0\rangle\langle 0| - |1\rangle\langle 1|$, $\bar{\sigma}_x = |1\rangle\langle 0| + |0\rangle\langle 1|$. Define the bare CPB Hamiltonian as

$$H_{\text{CPB}} = -2E_C(1 - 2n_g^{(0)})\bar{\sigma}_z - \frac{E_J}{2}\bar{\sigma}_x \quad (11.54)$$

and diagonalise it as

$$H_{\text{CPB}} = \frac{\varepsilon}{2}\sigma_z \quad (11.55)$$

where

$$\varepsilon = \sqrt{E_J^2 + [4E_C(1 - 2N_g^{(0)})]^2} \quad (11.56)$$

and now the Hamiltonian takes the form,

$$H = \hbar\omega_a a^\dagger a + \frac{\varepsilon}{2}\sigma_z - 4E_C\delta\hat{n}_g(t)[1 - 2n_g^{(0)} - \cos\theta\sigma_z + \sin\theta\sigma_x] \quad (11.57)$$

where we have now included the free Hamiltonian for the microwave cavity field, and

$$\theta = \arctan \left(\frac{E_J}{4E_C(1 - 2n_g^{(0)})} \right) \quad (11.58)$$

Operating at the charge degeneracy point, $n_g^{(0)} = 1/2$ so that $\theta = \pi/2$, the Hamiltonian becomes

$$H = \hbar\omega_c a^\dagger a + \frac{\varepsilon}{2} \sigma_z - 4E_C \frac{C_g}{2e} \hat{v}(t) \sigma_x \quad (11.59)$$

$$= \hbar\omega_c a^\dagger a + \frac{\varepsilon}{2} \sigma_z - \hbar g (a + a^\dagger) \sigma_x \quad (11.60)$$

where the coupling constant is

$$\hbar g = e \frac{C_g}{C_\Sigma} \sqrt{\frac{\hbar\omega_r}{Lc}} \quad (11.61)$$

This can be as large as 50 MHz [13]. The circuit resonance is typically at $\omega_c \approx 1$ GHz. However, we can detune the qubit from this resonant frequency by a few MHz [14]. We can then make the rotating wave approximation and take the Hamiltonian in the interaction picture to be the usual Jaynes–Cummings form

$$H_I = \hbar\delta_a a^\dagger a + \hbar g (a\sigma_+ + a^\dagger\sigma_-) \quad (11.62)$$

with $\delta_a = \omega_c - \omega_b$ is the detuning between the cavity resonance and the CPB and $\hbar\omega_b = \varepsilon$.

Exercises

11.1 A laser may be modeled by the master equation in (11.34) with $\varepsilon = 0$ and with the addition of the incoherent pump term

$$\mathcal{L}_P \rho = \frac{r}{2} \sum_{j=1}^N (2\sigma_+^{(j)} \rho \sigma_-^{(j)} - \sigma_-^{(j)} \sigma_+^{(j)} \rho - \rho \sigma_-^{(j)} \sigma_+^{(j)}) \quad (11.63)$$

We will also assume that $\omega_A = \omega_c$

(a) Show that the Fokker–Planck equation is now given by

$$\begin{aligned} \frac{\partial P}{\partial t} = & [-\partial_\alpha [-\kappa\alpha/2 - igv] - \partial_v [ig\alpha D - \gamma_\parallel v/2] \\ & - \partial_D [-\gamma_\parallel (D - D_0) - 2ig(u\alpha - v\beta)] \\ & + \partial_v^2 [ig\alpha v] - 2r \frac{\partial^2}{\partial v \partial D} + NP \frac{\partial^2}{\partial v \partial u} \\ & + \partial_D^2 [r(N - D) + \gamma(D + N) - 2ig(u\alpha - v\beta) + CC] P \end{aligned} \quad (11.64)$$

where $\gamma_{\parallel} = \gamma + r$ and

$$D_0 = N \left(\frac{r - \gamma}{r + \gamma} \right) \quad (11.65)$$

(b) By considering the deterministic equations of motion show that laser action requires $D_0 > 0$.

(c) Show that the steady state field amplitude obeys the equation

$$x \left(1 - \frac{C_1}{1 + |x|^2} \right) = 0 \quad (11.66)$$

where $x = \alpha / \sqrt{n_0}$ with

$$n_0 = \frac{\gamma \gamma_{\parallel}}{8g^2} \quad (11.67)$$

$$C_1 = \frac{4g^2 D_0}{\gamma_{\parallel} \kappa} \quad (11.68)$$

(d) Define $I = |x|^2$. Show that the stable solutions are

$$I = \begin{cases} 0 & \text{if } C_1 < 1 \\ C_1 - 1 & \text{if } C_1 > 1 \end{cases} \quad (11.69)$$

References

1. R. Miller, T.E. Northrop, K.M. Birnbaum, A. Boca, A.D. Boozer, H.J. Kimble: J. Phys. B: At. Mol. Opt. Phys. **38**, s551 (2005)
2. J. Ye, D.W. Vernooy, H.J. Kimble: Phys. Rev. Lett. **83**, 4987 (1999)
3. T. Puppe, I. Schuster, A. Grothe, A. Kubanek, K. Murr, P.W.H. Pinsky, G. Rempe: quant-ph/072162 (2007)
4. M. Keller, B. Lange, K. Hayasaka, W. Lange, H. Walther: Nature **431**, 1075 (2004)
5. K. Fortier, S.Y. Kim, M.J. Gibbons, P. Ahmadi, M.S. Chapman: Phys. Rev. Lett. **98**, 233601 (2007)
6. T. Aoki, B. Dayan, E. Wilcut, W.P. Bowen, A.S. Parkins, H.J. Kimble: Nature, **443**, 671 (2006)
7. K. Hennessy, A. Badolato, M. Winger, D. Gerace, M. Attüre, S. Gulde, S. Fält, E.L. Hu, A. Imamoglu: Nature **445**, 896 (2007)
8. J.M. Raimond, M. Brune, S. Haroche: Rev. Mod. Phys. **73**, 565 (2001)
9. A. Boca, R. Miller, K.M. Birnbaum, A.D. Boozer, J. McKeever, H.J. Kimble: Phys. Rev. Lett. **93**, 233603 (2004)
10. A. Kirag, M. Attüre, A. Imamoglu: Phys. Rev. A., **69**, 032305 (2004)
11. M.J. Fernee, H. Rubinsztein-Dunlop, G.J. Milburn, Phys. Rev. A., **75**, 043815 (2007)
12. P.D. Drummond, D.F. Walls: Phys. Rev. A **23**, 2563 (1981)
13. A. Blais, R. Huang, A. Walraff, S. Girvin, R.J. Schoelkopf: Phys. Rev. A **69**, 062320 (2004)

14. D.I. Schuster et al.: Nature **445**, 515 (2007)
15. J.F. Annett, B.L. Gyorffy, T.P. Spiller: *Superconducting Devices for Quantum Computation*. In 'Exotic States in Quantum Nanostructures', S. Sarkar (ed.) (Kluwer Academic Publishers 2002)

Further Reading

Haroche, S., J.M. Raimond: *Exploring the quantum* (Oxford University Press, Oxford, UK 2006)